Accepted Manuscript

Insight into the immobilization of ionic liquid on porous carbons

M. Rufete-Beneite, M.C. Román-Martínez, A. Linares-Solano

Please cite this article as: Rufete-Beneite, M., Román-Martínez, M.C., Linares-Solano, A., Insight into the immobilization of ionic liquid on porous carbons, *Carbon* (2014), doi: http://dx.doi.org/10.1016/j.carbon. 2014.06.009

Insight into the immobilization of ionic liquid on porous carbons

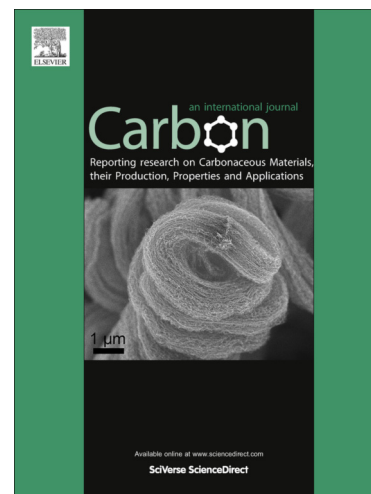M. Rufete-Beneite, M.C. Román-Martínez*, A. Linares-Solano

Departamento de Química Inorgánica e Instituto de Materiales. Universidad de Alicante. Apdo. 99. E-03690 Alicante. España.

*Corresponding author
Tel. 0034965903975, Fax: 0034965903454
e-mail: mcroman@ua.es

Abstract

Very different carbon materials have been used as support in the preparation of Supported Ionic Liquid Phase samples (SILP). Some of them have been oxidized, either strongly (with ammonium persulfate solution) or weakly (with air at 300 ºC, 2h). The purpose is to establish which properties of the supports (e.g., porosity -volume and type-, surface area, oxygen surface chemistry and morphology) determine the IL adsorption capacity and the stability (immobilization) of the supported IL phase. The ionic liquid used in this work is 1-butyl-3-methyl-imidazolium hexafluorophosphate ([bmim][PF$_6$]). For each support, samples with different amounts of ionic liquid have been prepared. The maximum IL that can be loaded depends mainly on the total pore volume of the supports. For comparable pore volumes, the porosity type and the oxygen surface content have no influence on the IL loading. The supported IL fills most of the pores, leaving some blocked porosity. The stability of the supported IL phase (especially important for its subsequent use in catalysis) has been tested in water under general hydrogenation conditions (60 °C and 10 bar H$_2$). In general, leaching is low but it increases with the amount of IL loaded and with the oxidation treatments of the supports.

1. Introduction

Ionic liquids (ILs) are low melting point salts that have interesting properties as solvents because of their negligible vapor pressures and the ability of solving many different substances. Besides, the wide range of possible combinations of cations and anions implies that other solvent properties may be easily controlled. Hence, there is currently great interest in the use of ILs for many applications, including catalysis [1-10]. In particular, applications of ILs in the chemical industry have been recently reported [11]. Immobilization of ILs on solid supports may improve their applicability in industrial processes. Preparation of a supported ionic liquid phase (SILP) on several polymeric [12, 13] and inorganic supports [14-16] has been the subject of several recent research works.

In the field of catalysis, SILP systems (known as SILC (supported ionic liquid catalysis)) are particularly interesting due to several attractive advantages, which, as indicated by Selvam et al. [16], are: (i) concomitant use of ILs, (ii) high catalytic activity owing to a uniform distribution of catalytic active species within the SILP, and (iii) easy separation from the reaction products for further reusability.

Although less investigated, carbon materials are, as well, suitable supports for SILP systems in general, and for SILC systems in particular. This is because they can be prepared with large surface areas, tuned porosity and variable surface chemistry. This allows, thus, a broad variety of arrangements and interactions of the IL within the support surface. There are some works dealing with SILP systems based on carbon materials using for example a carbon cloth [17, 18], carbon nanofibres that cover sintered metal fibres [19], commercially available mesoporous and microporous carbon beads [20], commercial activated carbons [21] and carbon nanotubes [22-25].

Beyond the development of SILP catalytic systems, the adsorption of IL on carbon materials has potential uses in other application areas like EDLC (Electric Double-Layer Capacitors) or the removal of IL from aqueous effluents, in which activated carbon has been used [26].

Understanding the adsorption process and the interactions of ionic liquid with carbon materials is of the outermost importance to develop applications of carbon based SILP

3

systems, and thus, it is very interesting to determine the effect that the carbon characteristics might have on the supported ionic liquid. Besides, it should be taken into account that most of works dealing with SILP systems define them as an "adsorbed film" or as a "coated surface". However, in the particular case of porous carbon supports, it must be analyzed if the supported IL constitutes a film or it fills the porosity.

Lemus et al. [21] have addressed the topic of carbon based SILP systems using three commercial activated carbons. After a complete characterization of supports and SILP samples, they conclude that there is a relationship between the total pore volume and the IL loading and a negative effect of the support acidity on the thermal stability of the SILP sample.

The present work deals with the preparation of SILP samples using as support several carbon materials of very different surface area, pore structure (volume and type), surface chemistry and morphology. The purpose is to establish which of the mentioned properties of the support determine its IL adsorption capacity and the stability (immobilization) of the supported IL phase, especially for a subsequent use in the field of catalysis in liquid phase.

2. Experimental

2.1. Carbon materials

To cover a wide range of support properties (porosity, surface chemistry and morphology) the following carbon materials have been used in this work:

GeA: Spherical shaped activated carbon material prepared from a phenolic resin by Gun-ei Chemical Industry (Japan). The spheres have an average diameter of 150 µm.

KA: Spherical shaped activated carbon material produced from petroleum pitch by Kureha Corporation (Japan). The spheres have an average diameter of 780 µm.

T: Carbon black T-10157 from Columbian Chemical Company (USA).

SA: Powder activated carbon SA-30 from MeadWestvaco (USA).

BPS: Activated carbon produced from an agricultural waste (Colombian banana pseudostem) by chemical activation with H_3PO_4 as described in [27].

C_{OH}: Functionalized multiwalled carbon nanotubes (obtained by CVD), purchased to Chengdu Organic Chemicals Co., Ltd, Chinese Academy of Sciences. They have the following average dimensions: outer diameter 10-20 nm, inner diameter 5-10 nm and length 10-30 µm. Purity is higher than 95% and the –OH content is 3.06 wt%.

4

Spherical carbon materials (GeA and KA) have been oxidized in order to modify their oxygen surface chemistry, and to analyze the importance of this variable. Two different oxidation procedures have been used: treatment with a saturated solution of ammonium persulfate $(NH_4)_2S_2O_8$ in sulfuric acid 1M for 24 h at room temperature (samples named GeAS and KAS); and treatment with air flow in a conventional horizontal furnace at 300°C for 2 h (samples named GeAOx2 and KAOx2).

2.2. Characterization of carbon materials

The carbon materials (CMs) have been characterized by gas adsorption (N_2 at -196 °C and CO_2 at 0 °C) using an Autosorb 6-B apparatus. Samples were previously degassed in vacuum at 150 °C for 5 h. N_2 adsorption data have been used to calculate the surface area by the BET method, the volume of micropores ($V_{\mu p}$) by applying the Dubinin-Radushkevich equation and the volume of mesopores (up to 7 nm, V_{meso}) assessed as the difference between the adsorbed volume of N_2 at P/P^0=0.99 and at P/P^0=0.2 [28, 29]. CO_2 adsorption data have been used to calculate the volume of narrow micropores [30, 31] (pore smaller than 0.7nm, $V_{n\mu p}$) by applying the Dubinin-Radushkevich equation.

The effect of the oxidation treatments carried out has been analyzed by determining the amount of oxygen surface groups present in both, the pristine and the oxidized CMs. Such analysis has been assessed by temperature programmed desorption experiments [32-34] under the following conditions: the samples were heated in helium flow (100 cm^3/min) at 10 °C/min up to 1000 °C in a thermobalance TG-DTA (Mettler Toledo) coupled to a mass spectrometer (Thermostar GSD301T of Pfeiffer Vacuum). In this way, the mass loss due to decomposition of surface oxygen groups and the simultaneous evolution of CO and CO_2 have been recorded.

2.3 Preparation of IL/CM samples

The ionic liquid used in this work is 1-butyl-3-methyl-imidazolium hexafluorophosphate ([bmim][PF$_6$]) supplied by Solvionic. The molecular structure of this compound is shown in the scheme of Figure 1.
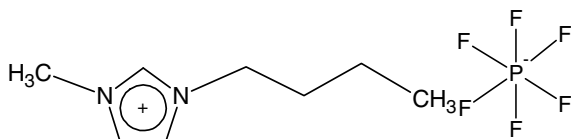

Figure 1. Molecular scheme of the ionic liquid [bmim][PF$_6$].

5

IL/CM samples with different IL loadings were prepared inside a Schlenk system. The procedure to support the ionic liquid on the carbon materials is as follows: about 0.5 g of the carbon material were degassed in vacuum at 150 °C for 5 h; after cooling, the desired amount of ionic liquid, mixed with 2 cm^3 of acetone, was added to the outgassed solid and the system was kept under Ar atmosphere and stirring until the sample took on a dry aspect. The maximum amount of IL accepted by each support was determined by repeating the above mentioned procedure until the sample loses the dry appearance. The name given to the IL/CM samples consists of the name of the carbon material and a number indicating the amount of ionic liquid loaded as wt%.

2.4 Characterization of IL/CM samples

The amount of ionic liquid loaded was determined by weighing samples before and after the IL loading. In several cases the loaded amount was also determined by elemental analysis (Microanalyzer Thermo Finnigan Flash 1112 elemental Series), through the N content, and by thermogravimetry (thermobalance TG-DTA (Mettler Toledo). Additionally, thermogravimetry was used to study the stability of the loaded ionic liquid. For TG measurements, the samples were heated in nitrogen flow (80 cm^3/min) at 10 °C/min up to 800°C.

All samples containing IL (IL/CM samples) were characterized by gas adsorption (N_2 at -196 °C and CO_2 at 0 °C). Gas adsorption measurements and data analysis were carried out as indicated previously in the case of supports.

2.5 Stability of the IL/CM samples in water

For application in heterogeneous catalysis, the stability of the supported IL under reaction conditions is absolutely necessary. Thus, this property has been tested as follows: the IL/CM sample (0.5 g) was put in a stainless steel reactor with 10 cm^3 of water at 60°C and 10 bar H_2 for 16 h (these are general hydrogenation conditions). After the indicated period of time, the liquid phase was separated by filtration and analyzed by UV-Vis spectroscopy (Jasco V-650) at 212 nm to determine the amount of IL leached. In some cases, the results obtained were contrasted with the amount of IL remaining in the IL/CM sample, measured by elemental analysis. As the concordance was good, UV-Vis spectroscopy was used generally.

3. Results and discussion

3.1. Characterization of CM samples

3.1.1. *Textural properties*

Figure 2 shows the N_2 adsorption isotherms at -196 °C of the starting carbon materials (Figure 2a) and the oxidized samples (Figure 2b). These isotherms reveal porosity developments and pore size distributions widely different in the series of materials selected for this study.
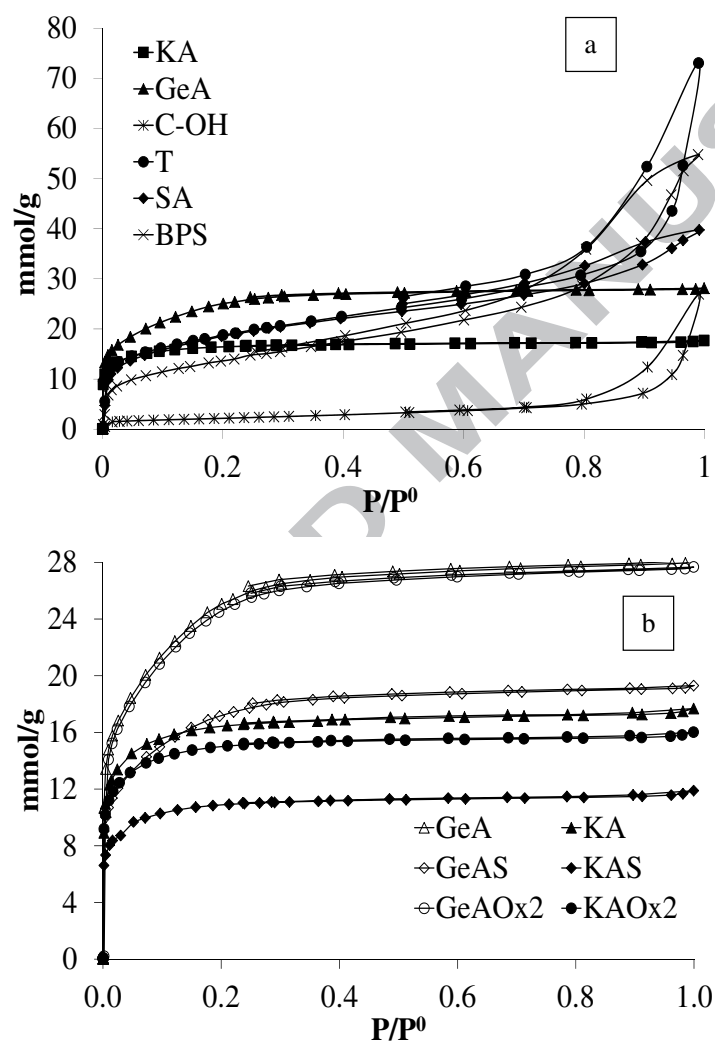

Figure 2. N_2 adsorption isotherms at -196 °C of the carbon materials: (a) original samples and (b) original and oxidized spherical carbon samples.

The N_2 adsorption isotherms of samples KA and GeA do not present hysteresis loop and they are type I according to the IUPAC classification, typical of microporous solids

7

[29]. The isotherms of samples T, SA and BPS are type I+IV, characteristic of samples with micro and mesoporosity [29] whereas the N_2 isotherm of sample C_{OH} is type II, indicating the formation of adsorbed layers and capillary condensation in mesopores. Table 1 shows a summary of some textural properties of the original carbon materials calculated from N_2 adsorption at -196 °C and CO_2 adsorption at 0 °C data as indicated in the experimental section.

Table 1. Textural properties of the carbon materials used as supports.

Sample	$S_{BET}(m^2/g)$	$V_{total}(cm^3/g)^a$	$V_{\mu p}(cm^3/g)^b$	$V_{n\mu p}(cm^3/g)^c$	$V_{meso}(cm^3/g)^d$
GeA	1918	0.98	0.83	0.50	0.11
GeAS	1351	0.67	0.58	0.41	0.08
GeAOx2	1968	0.96	0.77	0.47	0.11
KA	1291	0.67	0.55	0.44	0.11
KAS	809	0.41	0.39	0.32	0.03
KAOx2	1096	0.56	0.54	0.40	0.04
T	1491	2.53	0.60	0.34	1.88
SA	1494	1.38	0.62	0.30	0.74
BPS	1124	1.90	0.45	0.21	1.41
C_{OH}	176	0.93	0.07	0.04	0.86

[a]Total pore volume, determined by the amount adsorbed at $P/P^0=0.99$ in the N_2 adsorption isotherm at -196°C.
[b]Micropore volume calculated by the Dubinin-Radushkevich equation applied to the N_2 adsorption isotherm at -196°C.
[c]Narrow micropore (<0.7nm) volume calculated by Dubinin-Radushkevich equation applied to the adsorption isotherm of CO_2 at 0 °C.
[d]Mesopore volume calculated by the difference between the adsorbed volume of N_2 at $P/P^0=0.99$ and at $P/P^0=0.2$.

Data of Figure 2a and Table 1 confirm that the supports used in this work have a broad variety of textural properties. Samples KA and GeA are essentially microporous while samples T, SA and BPS contain a significant amount of both micro and mesopores. The carbon nanotubes, sample C_{OH}, can be considered as basically mesoporous.

Figure 2b shows the N_2 adsorption isotherms at -196 °C of the oxidized samples and for the sake of comparison the data corresponding to the original spherical carbon materials have been also included. Oxidation with the $(NH_4)_2S_2O_8$ solution produces a noticeable reduction of the adsorption capacity of both samples whereas contrarily, the oxidation with air does not produce changes in the adsorption isotherms (only a slight decrease in sample KA). Table 1, in which the textural characteristics of the oxidized samples are

8

also compiled, clearly shows the mentioned important decrease of the adsorption capacity caused by the oxidation with the $(NH_4)_2S_2O_8$ solution.

3.1.2. Oxygen surface chemistry

Figure 3 presents an example of the CO_2 and CO desorption profiles (Figures 3a and 3b, respectively) obtained in typical TPD experiment runs. This example corresponds to sample KA and the two oxidized samples obtained from it (samples KAS and KAOx2). The TPD profiles of the other samples are those expected according to the nature of the carbon materials and/or the activation methods and treatments used [34-38].The amounts of CO_2 and CO evolved (in μmol/g) have been assessed from the TPD profiles and data are collected in Table 2 together with the corresponding total amount of atomic oxygen (calculated from the amount of CO_2 and CO evolved) expressed as wt %. It can be seen that samples SA and BPS have a much higher amount of oxygen surface groups than the rest of samples. Such difference is expected considering that both samples have been prepared by phosphoric acid activation [27, 36].
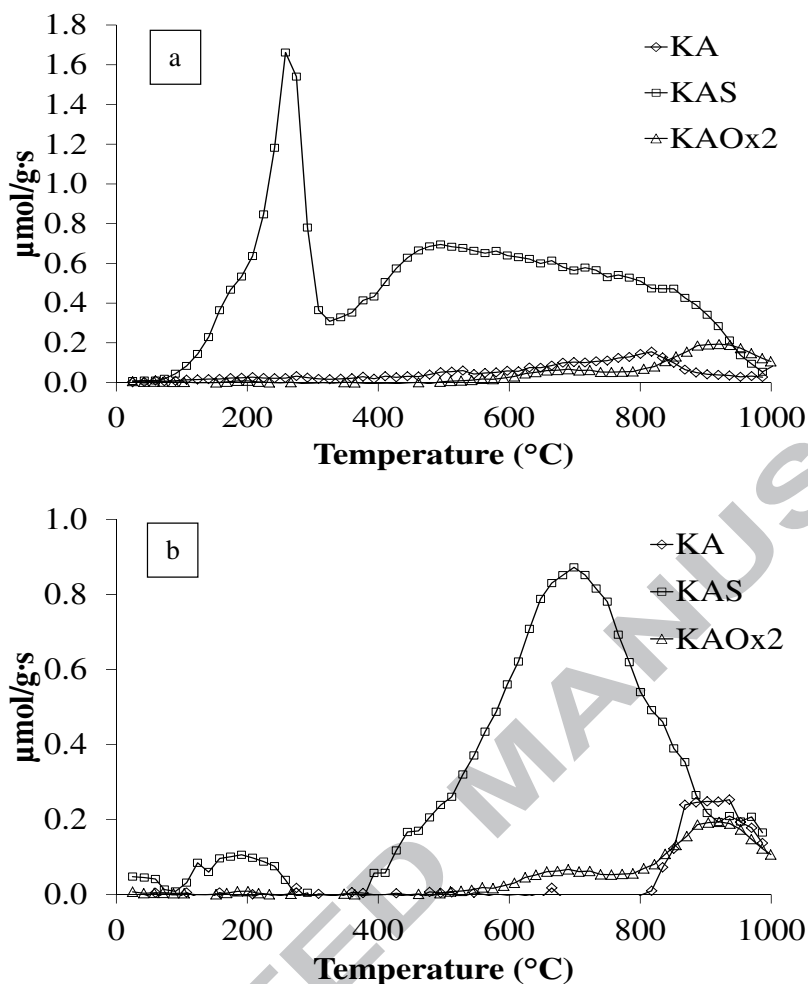
Figure 3. TPD profiles of samples KA, KAS and KAOx; (a) CO_2 and (b) CO (He (100 cm^3/min), 10 °C/min).

Table 2. Quantification of the TPD profiles

Sample	CO_2 (µmol/g)	CO (µmol/g)	O wt%
GeA	790	960	4
GeAS	3810	3105	17
GeAOx2	1227	612	5
KA	291	167	1
KAS	2903	1654	12
KAOx2	719	247	3
T	179	505	1
SA	404	1720	4
BPS	693	2678	6
C_{OH}	716	668	3

10

As expected, data of Figure 3 and Table 2 show that the oxidation treatments carried out increase the surface oxygen contents of the oxidized samples. However, both oxidizing treatments lead to very different surface chemistry; the treatment with the ammonium persulfate solution results to be much more drastic than the treatment with air (see the case of KA, Figure 3 and Table 2). Thus, the oxidation with ammonium persulfate solution, contrarily to what happens with air, produces a larger development of surface oxygen complexes in both samples and quite different CO_2 and CO evolution profiles (indicative of different oxygen functionalities) [32-34, 38]. Thus, it should be pointed out that the treatment with ammonium persulfate solution produces in both samples a selective formation of oxygen groups that decompose as CO_2 below 400 °C, evidenced by the sharp band centered at about 275 °C (Figure 3a) that is assigned to decomposition of carboxylic type groups [37, 38].The oxidizing treatment with air produces a much slight increase and modification of the oxygen surface groups that decompose as CO_2 above 500 °C (see Figure 3 and Table 2).

In summary, the oxygen surface chemistry of the supports used (starting samples and the oxidized ones) differs widely in, both, the surface oxygen content and the nature of these oxygen surface groups. Therefore, the series of samples used will allow analyzing the effect of the oxygen surface chemistry on the IL loading and on the stability of the IL/CM samples.

3.2. IL/CM samples

All IL/CM samples prepared are collected in Table 3, in which the amount of ionic liquid is expressed as total wt %, as gram per gram of sample, as cm^3 per gram of sample (using the density of the [bmim][PF$_6$] IL of 1.37 g/cm^3[39] and as the volume of ionic liquid related to total pore volume (dL (%)). As indicated before, data of Table 3 have been determined by the difference of the sample weight with and without loaded IL and, in some cases, these results have been contrasted with determinations by elemental analysis and TG measurements, and a good data concordance has been obtained, in agreement with [21].

The maximum amount of IL that can be loaded in a given sample (i.e., keeping a dry appearance) is identified in Table 3 by the underlined name. It can be seen that there are

samples with quite different maximum amounts of loaded IL: from 20 wt% to 70 wt%. As it will be discussed later, the highest amount of ionic liquid that can be loaded on a given carbon support depends on its porosity and co-relates very well with the sample pore volume.

Table3. Samples with different amount of IL, expressed as wt%, g(IL)/g(support), cm^3(IL)/g(support) and volume of IL related to the total pore volume(dL (%)).

Sample	wt%	g(IL)/g(support)	cm^3(IL)/g(support)	dL (%)[a]
GeA-30	30.12	0.43	0.31	32
GeA-40	40.06	0.67	0.49	50
GeA-50	49.98	0.99	0.73	74
GeAS-30	30.25	0.43	0.32	48
GeAS-40	40.82	0.69	0.50	75
GeAOx2-30	30.33	0.43	0.32	33
GeAOx2-40	39.9	0.66	0.48	50
GeAOx2-50	50.34	1.01	0.74	77
KA-20	20.35	0.25	0.19	28
KA-30	31.74	0.46	0.34	51
KA-40	40.58	0.68	0.50	75
KAS-20	20.06	0.25	0.18	44
KAOx2-30	32.3	0.46	0.34	61
KAOx2-40	40.4	0.69	0.49	88
T-40	41.90	0.72	0.53	21
T-75	74.65	2.95	2.15	85
SA-60	61.31	1.58	1.16	84
BPS-60	60.32	1.52	1.11	58
BPS-70	69.91	2.32	1.68	88
C_{OH}-3	2.75	0.02	0.02	2
C_{OH}-30	29.31	0.41	0.30	32
C_{OH}-40	40.06	0.67	0.49	53

[a] volume of ionic liquid loaded related to total pore volume of the support (see Table 1)

3.3 Characterization of IL/CM samples.

Thermogravimetric analysis has been used to assess the amount of ionic liquid loaded in samples of series GeA and KA and to analyze the thermal stability range of the supported IL. Figure 4a shows the TG profiles obtained for sample GeA with different amounts of IL. Similar TG profiles have been obtained for sample KA with different

12

amounts of IL. For all the samples studied, the onset temperature for the decomposition of the supported ionic liquid is around 400 °C, similar to the reported data for the same unsupported IL [40]. It must be mentioned that this parameter is very sensitive to the TG experimental conditions, and values that differ up to 50 °C can be obtained [40]. Interestingly, the IL weight-loss data assessed from TG profiles similar to those of Figure 4a, show that for samples of GeA and KA series the mass loss registered in the TG experiment agrees perfectly with the amount of ionic liquid determined by weight.

Figure 4b, that presents the TG profiles of IL/CM samples prepared with the highly oxidized support GeAS, shows that these TG curves are much more complex than those of Figure 4a. As the temperature increases a continuous weight loss takes place and the onset temperature is not as clear as in Figure 4a. Additionally, there is no agreement between the amount of loaded IL determined by weighing the sample with and without IL and the mass loss determined by TG. The TG profile of sample GeAS shows the mass loss due to the decomposition of surface oxygen complexes which agrees well with the amount of evolved H_2O, CO and CO_2 determined by mass spectrometry. For samples GeAS-30 and GeAS-40 this process overlaps with the decomposition of the supported IL and the registered mass loss does not correspond to the weight of the loaded IL (even considering the surface oxygen complexes evolved). As observed in Figure 4b, the total mass loss of samples GeAS-30 and GeAS-40 is similar in spite of having a different amount of IL (confirmed by elemental analysis and sample weight before and after IL loading). A similar complexity has also been found in the case of samples KAS and KAS-20, that is, samples oxidized with ammonium persulfate solution.
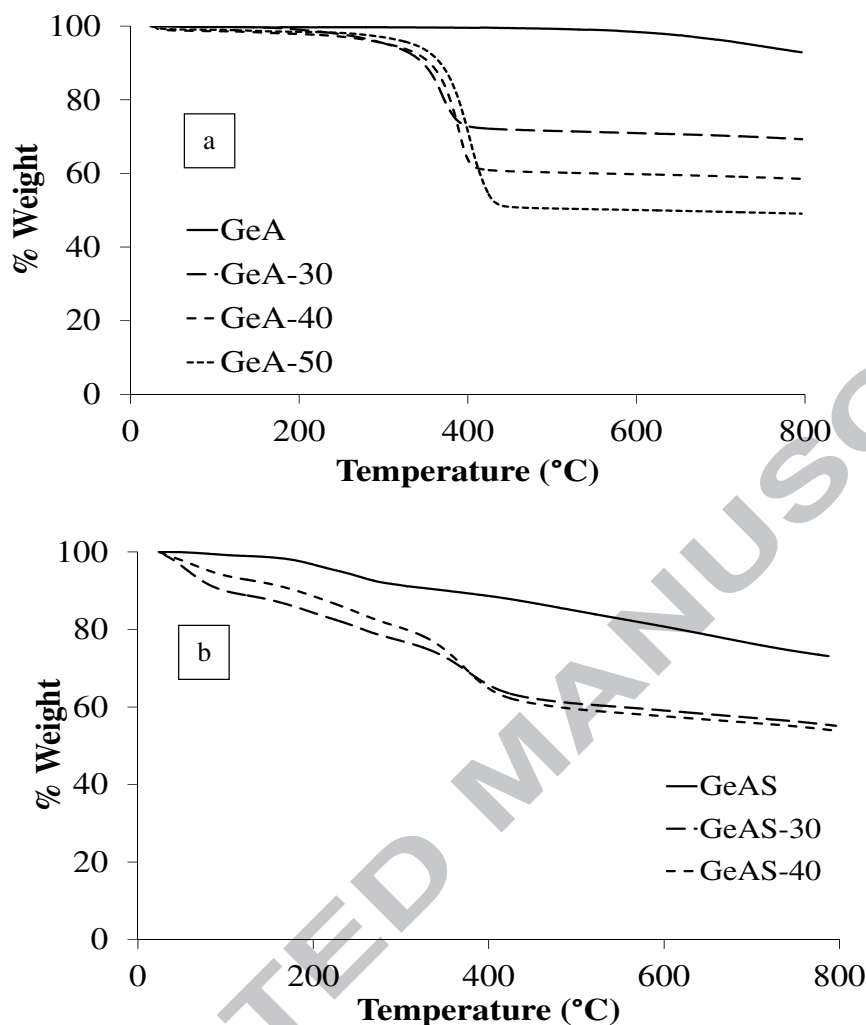
Figure 4. Thermogravimetric profiles of CM and IL/CM samples: (a) series GeA and (b) series GeAS (N_2 (80 cm^3/min), 10 °C/min).

Such a complexity could be related to the following observation: the glass container where these IL/CM samples (GeAS-30, GeAS-40 and KAS-20) were stored was somewhat damaged. Such damage was only observed with samples oxidized with ammonium persulfate solution and suggests that in these samples some corrosive substance that reacts with the glass container is generated. The corrosive substance is likely HF and it would be generated through the following reaction between the carboxylic surface groups and the PF_6^- anion (Figure 5):

Figure 5.Proposed reaction for the interaction between the PF_6^-anion of the ionic liquid and the surface carboxylic groups.

In this case, the interaction of the IL with the support surface would depend on the extent of the reaction shown in Figure 5 that would, as well, cause that the oxygen decomposition patterns (e.g., CO_2) be different, making more complex the TG profile and its interpretation. In any case, these TG profiles seem to confirm that such interaction between the ionic liquid and some surface oxygen groups takes places. Additionally, the fact that this effect has not been observed with other samples (including those oxidized with air) supports the proposed reaction with the carboxylic type oxygen groups.

Besides, it can be added that other modifications of the surface oxygen complexes by effect of IL could take place (for example dissociation of associated hydroxyl groups or dissolution of easily reductive groups) [41]; and also that reactions between IL and surface oxygen groups can occur under temperature programmed experiments. These facts contribute, as well, to the complexity of the TG profile.

The textural properties of all IL/CM samples have been assessed with N_2 adsorption to study the degree of porosity occupied by the IL as a function of the amount of IL loaded. Firstly, it should be mentioned that under the outgassing conditions used for these measurements, the loaded IL is stable and remains on the sample porosity. In all cases the nitrogen adsorption isotherms of IL/CM samples show a reasonable linear decrease of the adsorption capacity with the increase of the IL loading. As an example of such behavior, the N_2 adsorption isotherms obtained for the samples of GeA series (GeA-30, GeA-40 and GeA-50) is presented in Figure 6.
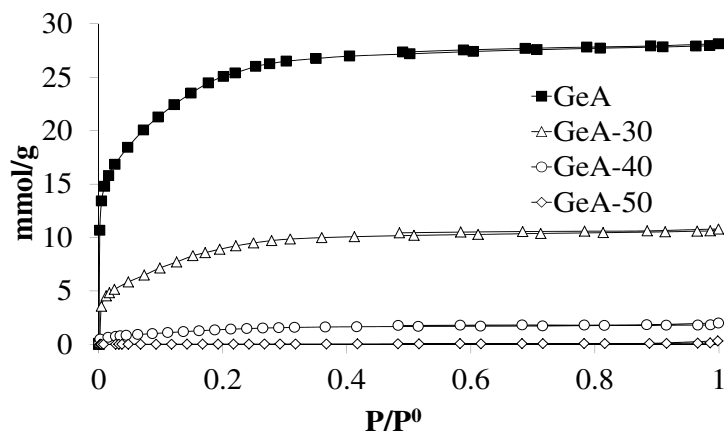
Figure 6.N_2 adsorption isotherms at -196 °C of IL/CM samples of series GeA.

As the IL loading increases, the adsorption capacity decreases and it becomes nil in the case of the maximum IL loading (sample GeA-50). A similar behavior is observed for all the other samples. The almost suppressed N_2 adsorption with the maximum IL loading suggests that the IL either completely fills the porosity or it produces some pore blockage. That is, depending on the amount of IL loaded, part of the pore volume might not be accessible to N_2, both because it is occupied by the ionic liquid and/or because the access of gases to some porosity is impeded by pore blockage.

3.4. Porosity of IL/CM samples with the highest IL loading.

Figure 7 presents the pore volume occupied by the maximum amount of loaded IL (using a density value of 1.37 g/cm^3) versus the total pore volume of the different supports studied (line a). This nice, and reasonable, correlation confirms the reliability of the procedure used to assess the maximum loading (keeping a dry appearance) which is only an approximate procedure.

It must be mentioned that a representation of the maximum volume of loaded IL against the BET surface area of supports does not lead to a correlation between both parameters. Thus, the significant textural parameter of supports is pore volume and not surface area.

In order to deep into the porosity of samples containing the maximum IL (assessed by N_2 adsorption), as well as into the reliability of Figure 7, the following data are collected in Table 4: Column-1) the total pore volume of the support and of the corresponding IL/CM sample (underlined name means sample with the maximum IL

16

loading); column-2) the "not accessible pore volume" calculated as the total pore volume of the support minus the total pore volume of the IL/CM sample; column-3) the volume of the loaded IL (see Table 3); and column-4) "blocked porosity" calculated as follows: the "not accessible pore volume" (column 2) minus the volume of the loaded IL in each IL/CM sample (column 3). The blocked porosity is expressed as an absolute value in cm^3/g and as % of the total pore volume of the support (in brackets). For this calculation it has been assumed that the IL volume does not change under the conditions of N_2 adsorption (-196 °C). This is an assumption because, in fact, as reported in the literature [42], when the ionic liquid [bmim][PF_6] is quickly cooled to the liquid nitrogen temperature it becomes an amorphous solid or glass. It has been also observed [42] that the solid IL shows a substantial degree of order even in their amorphous states, which resembles the crystalline order. Published data of crystalline [bmim][PF_6] give density values of about 1.50 g/cm^3[43]. Blocked porosity could be also calculated with the volume of loaded IL determined with 1.50 g/cm^3 instead of 1.37 g/cm^3giving higher values (from 20% to 60% of the total pore volume). However, data in Table 4 (calculated with d=1.37 g/cm^3) allow to have a closer view of the samples at room temperature.

Table 4. Analysis of pore filling in IL/CM samples with the highest IL loading.

Sample	1 Total pore volume (cm^3/g)	2 Not accessible pore volume (cm^3/g)	3 Loaded IL volume (cm^3/g)	4 Blocked porosity (cm^3/g)
GeA	0.98		-	
GeA-50	0.01	0.97	0.73	0.24 (24%)
GeAS	0.67		-	
GeAS-40	0.01	0.66	0.50	0.16 (24%)
GeAOx2	0.96		-	
GeAOx2-50	0.01	0.95	0.74	0.21(22%)
KA	0.67		-	
KA-40	0.01	0.66	0.50	0.16 (24%)
KAS	0.41		-	
KAS-20	0.02	0.39	0.18	0.21 (51%)
KAOx2	0.56		-	
KAOx2-40	0.01	0.55	0.49	0.06 (11%)
T	2.53		-	
T-75	0.01	2.52	2.15	0.37 (15%)
SA	1.38		-	
SA-60	0.02	1.36	1.16	0.20 (14%)

	1	2	3	4
BPS	1.90		-	
BPS-70	0.03	1.87	1.68	0.19 (10%)
C_OH	0.93		-	
C_OH-40	0.03	0.90	0.49	0.41(44%)

1- Total pore volume, determined by the amount adsorbed at P/P^0=0.99 in the N_2 adsorption isotherm at -196°C

2- Pore volume not accessible to N_2 determined as total pore volume of support CM minus total pore volume of sample IL/CM (underlined name means sample with the highest IL loading).

3- Amount of IL in samples IL/CM (data from Table 3).

4- Calculated by difference of columns 2 and 3. In brackets: percentage of the support total pore volume, that is (blocked porosity (cm^3/g)/support total pore volume (cm^3/g))*100

Assuming that the "dry appearance" procedure used to determine the maximum amount of IL is reliable and that the volume of the IL will not change during the N_2 adsorption due to the low temperature used (-196 °C), the following comments can be extracted from data of Table 4:

- In general, the "not accessible pore volume" is very similar to the total pore volume of the parent support confirming that the samples have been almost filled with the IL without losing the dry aspect.

- The maximum IL loading depends on the total pore volume, regardless the isotherm shape (type I or type IV), that is, independently of the type of porosity and of the pore size distribution.

- In all cases there is some blocked porosity, that is, porosity not occupied by IL but not accessible to the gaseous adsorbate. The blocked pore volume varies for the different supports.

- In general, the effect of the oxidation treatments is manifested through the porosity variation produced, that is, the reduction of the pore volume leads to a lower IL loading. However, in the case of sample KAOx2-40, the blocked porosity is less than in the original support, while in sample KAS-20 it is much higher. This effect can be due to some effect of the surface chemistry, which in the latter (ammonium persulfate oxidation) is quite different and can even produce additional changes in the pore structure.

- The presence of blocked porosity means that the IL could not form a continuous layer on the support inner surface.

18

Palomar et al.[26] already proposed the presence of blocked porosity in the case of IL adsorbed (from aqueous effluents) in a commercial activated carbon.

Figure 7 (line b) also shows a graphical representation of the not accessible pore volume of IL/CM samples versus the total pore volume of the different supports.

From these two graphical lines it can be stated that the non accessible pore volume is, for most of the samples, practically coincident with the total pore volume, meaning that the samples are effectively loaded with the IL. The maximum amount of loaded IL (in volume) follows a very linear relationship with the total pore volume. The difference between the two depicted point series corresponds to the blocked porosity.
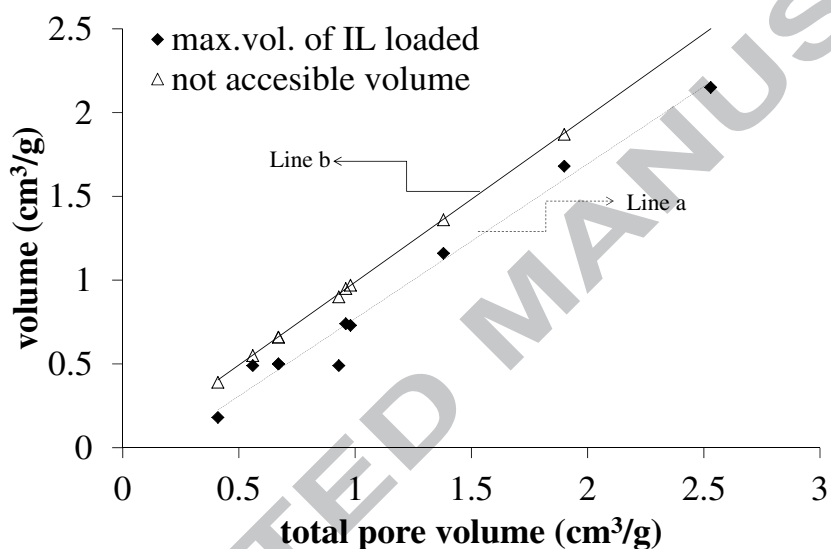

Figure 7. Volume of loaded IL and "not accessible pore volume" in samples IL/CM (data taken from Table 4, that is with loaded IL volume calculated with d=1.37 g/cm^3) versus the total pore volume of the support.

There are two samples with a significant relative amount of blocked porosity (Table 4): KAS-20 (51%) and C_{OH}-40 (44%). In the case of the carbon nanotubes, it can be explained by the particularity of the pore structure in which the tubular channels are likely not filled. On the other hand, sample KAS is essentially microporous and the extensive surface chemistry can partially hinder the access of the ionic liquid to the narrow porosity.

3.5. Porosity filling in samples with IL loadings lower than the maximum one

Samples with an IL loading lower than the maximum one have been also characterized by gas adsorption. Blocked porosity has been determined by data analysis similar to the one presented above. Figure 8 shows the calculated blocked porosity (as % of the total

pore volume of the support) of IL/CM samples with the highest IL loading and those of the same series with the immediately lower loading.
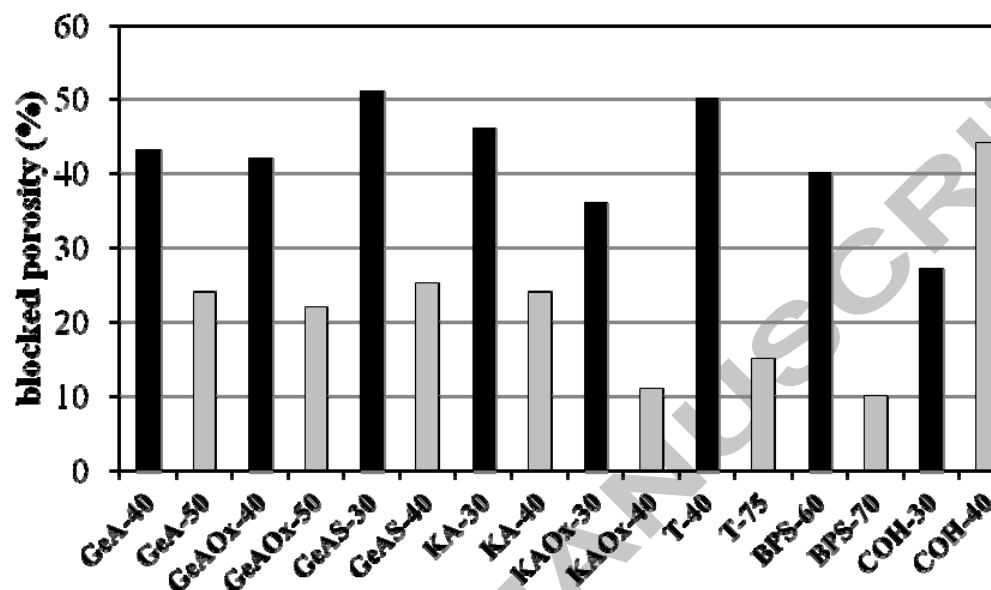

Figure 8.Blocked porosity in IL/CM samples with the two highest IL loadings (blocked porosity calculated from N_2 adsorption data and volume of loaded IL calculated with d=1.37 g/cm^3).

It has to be noted that in all cases, except in carbon nanotubes, the blocked porosity decreases with increasing the IL loading. This observation, contrarily to what would be expected, indicates that as more IL is loaded, it is forced to better penetrate into the sample porosity, leading to a lower blocked porosity. In the case of sample C_{OH}, however, as the amount of loaded IL increases more pores became blocked.

3.6.   Stability of the IL/CM samples in water

The main objective of this study is to analyze the stability of the IL/CM samples against leaching as a function of the different variables investigated (carbon material, type of porosity, oxygen surface chemistry and amount of IL). The stability of the IL/CM samples against leaching was tested in conditions similar to those used in catalytic activity tests (see experimental section) because these SILP systems are being used to immobilize a homogeneous catalyst, preparing thus a hybrid catalyst [44].

20

Samples of series KA have been selected to analyze the effect of aspects like the amount of IL loaded and the support oxidation and then, some other samples have been also investigated with the purpose of analyzing the effect of the support textural properties.

Table 5 shows a summary of the obtained results, where the amount of leached IL is expressed as % of the loaded amount and as the concentration of IL in the water phase, as wt %, after the stability test.

Table 5. Ionic liquid leached from different IL/CM samples (% of the original loading) and [IL] in water (wt%).

Entry	Sample	Leached IL (%)	[IL] in water (wt%)[a]
1	KA-20	1.4	0.01
2	KA-30	4.5	0.05
3	KA-40	12.9	0.25
4	KAS-20	23.8	0.24
5	KAOx2-40	19.3	0.75
6	GeA-20	3.4	0.02
7	GeA-40	11.4	0.23
8	GeAS-40	38.5	0.46
9	T-40	16.3	0.31
10	C_{OH}-40	92	1.8

[a] Calculated from the leached IL (%) considering the wt% of IL in the original IL/CM sample (Table 3) and 10 cm^3 of water used in the leaching tests.

Data of Table 5 can be analyzed as follows:

Regarding the effect of the IL loading, data obtained with the IL/KA samples show that the extent of leaching depends on the amount of IL loaded. Thus, leaching is very low for sample KA-20 and for sample KA-40 it is higher than 12%. The same appreciation results by comparing samples GeA-20 and GeA-40.

Regarding the effect of the oxidation treatment, it can be stated that it does not help to stabilize the supported IL; both oxidation treatments make the IL/CM sample more unstable against leaching (compare entries 4 and 5 with entries 1 and 3, respectively; and also entry 8 with entry 7). The oxidation with the ammonium persulfate aqueous solution that produces an extensive surface oxidation reduces the stability of the IL/CM samples against leaching; and the oxidation with air, that modifies the surface chemistry

21

and the porous texture only slightly, surprisingly leads, as well, to an important decrease of stability (compare entries 5 and 3). This behavior can be explained by a weaker interaction of the hydrophobic IL with a more hydrophilic support surface together with the favored interaction of water with a hydrophilic surface that displaces adsorbed hydrophobic species.

Regarding the effect of the nature and porosity of the carbon material it has been observed that the stability is more dependent on the amount of loaded IL than on the porosity of the carbon used. Thus, samples with very different porosities but with comparable IL loadings (e.g., KA-40, GeA-40 or T-40) have comparable leaching values. Especially interesting is the fact that sample T-40, prepared with a support having a larger volume of mesopores, shows the same stability, which allows concluding that the IL is retained similarly by micro- and mesoporosity.

Regarding the behavior of sample C_{OH}-40, it has been observed that the particular porous structure (external mesoporosity), morphology and size of support C_{OH}, leads to a very high leaching, revealing a very weak interaction of the IL with the surface of this carbon material, supporting, thus, the idea that the IL has no access to the tubular inner cavity.

Leaching of IL from the carbon porosity can be explained considering the affinity of the IL for both, the support, in which the liquid-solid equilibrium is involved, and for the solvent, determined by the liquid-liquid equilibrium.

Regarding the liquid-solid equilibrium two aspects must be considered: i) likely the IL loading of some samples is higher than that corresponding to the equilibrium. For example, Palomar et al. [26] have found that the adsorption capacity of a commercial activated carbon of 927 m^2/g for [bmim][PF_6] from an aqueous solution is about 1 mmol/g, which corresponds to only 0.21 cm^3/g. ii) As reported by the same authors [26], the adsorption capacity of an activated carbon for ILs in aqueous solution decreases as the temperature increases. As the temperature of the stability test (60 °C) is higher than the one used in the preparation (room temperature), the equilibrium amount of adsorbed IL is lower in the first case.

Studies of liquid-liquid equilibrium of water with [bmim][PF_6] [45] show that the concentration of IL in the aqueous phase at 25, 35 and 50 °C is 2.0, 2.2 and 2.7 wt%, respectively. Consequently, under the test conditions used to measure the stability of the IL/CM samples (0.5 g of IL/CM in 10 cm^3 water), samples with IL loadings equal to 20, 30 and 40 %, could suffer a 100% leaching, leading to concentrations in the aqueous

22

phase of about 1, 1.6 and 2 wt%, respectively. That means, based on the mentioned liquid-liquid equilibrium data, that a 100% leaching could take place, but, and importantly, this does not happen (see Table 5) revealing that the interaction of the IL with the porous support has an important effect.

In any case, as for application in catalysis leaching has to be negligible, it is necessary to look for an even more stable system, in which the interaction of the IL with the support be stronger, like that achieved with a covalent anchoring.

4. Conclusions

The immobilization of the ionic liquid [bmim][PF$_6$] (1-butyl-3-methyl-imidazolium hexafluorophosphate) on porous carbon materials has been investigated using a series of supports with a broad variety of textural, chemical and morphological properties. Some of them have been oxidized, either strongly (with ammonium persulfate solution) or weakly (with air at 300 ºC, 2h). The maximum amount of IL that can be loaded depends on the total pore volume of the supports, and neither the porous structure nor the oxygen surface chemistry play a significant role. N$_2$ adsorption data reveal that IL/CM samples with the highest IL loading do not have accessible pore volume meaning that, in fact, the maximum loading has been reached. With the investigated loadings, the supported IL largely fills the pores, but leaves some blocked porosity; and the system should not be considered as a supported film. Leaching in water under general hydrogenation conditions is in general low, but it increases with the amount of IL loaded. The oxidation treatments of the supports lead to less stable samples.

Acknowledgements

References

[1]. A. Kokorin; *Ionic Liquids: Applications and Perspectives*, In Tech (2011)

[2]. C. M. Gordon; *New developments in catalysis using ionic liquids*, Applied Catalysis A: General **222** (2001) 101-117.

[3]. Y. Gu, G. Li; *Ionic liquids-based catalysis with solids: State of the art*, Advanced Synthesis and Catalysis **351** (2009) 817-847.

[4]. J. P. Hallett, T. Welton; *Room-temperature ionic liquids: Solvents for synthesis and catalysis. 2*, Chemical Reviews **111** (2011) 3508-3576.

[5]. H. Olivier-Bourbigou, L. Magna, D. Morvan; *Ionic liquids and catalysis: Recent progress from knowledge to applications*, Applied Catalysis A: General **373** (2010) 1-56.

[6]. T. Welton; *Room-Temperature Ionic Liquids. Solvents for Synthesis and Catalysis*, Chemical Reviews **99** (1999) 2071-2084.

[7]. P. Wasserscheid, T. Welton (eds); *Ionic Liquids in Synthesis*, Wiley-VCH (2002)

[8]. P. Wasserscheid, W. Keim; *Ionic Liquids New Solutions for Transition Metal Catalysis*, Angewandte Chemie International Edition **39** (2000) 3772-3789.

[9]. C. H. Vasile I.Pârvulescu; *Catalysis in Ionic Liquids*, Chemical Reviews **107** (2007) 2615-2665.

[10]. M. Haumann, A. Riisager; *Hydroformylation in Room Temperature Ionic Liquids (RTILs): Catalyst and Process Developments*, Chemical Reviews **108** (2008) 1474-1497.

[11]. N. V. Plechkova, K. R. Seddon; *Applications of ionic liquids in the chemical industry*, Chemical Society Reviews **37** (2008) 123-150.

[12]. L. Han, H. J. Choi, D. K. Kim, S. W. Park, B. Liu, D. W. Park; *Porous polymer bead-supported ionic liquids for the synthesis of cyclic carbonate from CO_2 and epoxide*, Journal of Molecular Catalysis A: Chemical **338** (2011) 58-64.

[13]. V. Sans, F. Gelat, N. Karbass, M. I. Burguete, E. García-Verdugo, S. V. Luis; *Polymer cocktail: A multitask supported ionic liquid-like species to facilitate multiple and consecutive C-C coupling reactions*, Advanced Synthesis and Catalysis **352** (2010) 3013-3021.

[14]. C. P. Mehnert; *Supported ionic liquid catalysis*, Chemistry - A European Journal **11** (2005) 50-56.

[15]. A. Riisager, R. Fehrmann, M. Haumann, P. Wasserscheid; *Supported ionic liquids: Versatile reaction and separation media*, Topics in Catalysis **40** (2006) 91-102.

[16]. T. Selvam, A. MacHoke, W. Schwieger; *Supported ionic liquids on non-porous and porous inorganic materials - A topical review*, Applied Catalysis A: General **445-446** (2012) 92-101.

[17]. J. P. Mikkola, J. Wärnå, P. Virtanen, T. Salmi; *Effect of internal diffusion in supported ionic liquid catalysts: Interaction with kinetics*, Industrial and Engineering Chemistry Research **46** (2007) 3932-3940.

[18]. J. P. Mikkola, P. P. Virtanen, K. Kordás, H. Karhu, T. O. Salmi; *SILCA-Supported ionic liquid catalysts for fine chemicals*, Applied Catalysis A: General **328** (2007) 68-76.

[19]. M. Ruta, I. Yuranov, P. J. Dyson, G. Laurenczy, L. Kiwi-Minsker; *Structured fiber supports for ionic liquid-phase catalysis used in gas-phase continuous hydrogenation*, Journal of Catalysis **247** (2007) 269-276.

[20]. E. J. García-Suárez, P. Moriel, C. Menéndez-Vázquez, M. A. Montes-Morán, A. B. García; *Carbons supported bio-ionic liquids: Stability and catalytic activity*, Microporous and Mesoporous Materials **144** (2011) 205-208.

[21]. J. Lemus, J. Palomar, M. A. Gilarranz, J. J. Rodríguez; *Characterization of Supported Ionic Liquid Phase (SILP) materials prepared from different supports*, Adsorption **17** (2011) 561-571.

[22]. M. Tunckol, J. Durand, P. Serp; *Carbon nanomaterial-ionic liquid hybrids*, Carbon **50** (2012) 4303-4334.

[23]. M. J. Park, J. K. Lee, B. S. Lee, Y. W. Lee, I. S. Choi, S. g. Lee; *Covalent Modification of Multiwalled Carbon Nanotubes with Imidazolium-Based Ionic Liquids: Effect of Anions on Solubility*, Chemistry of Materials **18** (2006) 1546-1551.

[24]. J. Y. Shin, Y. S. Kim, Y. Lee, J. H. Shim, C. Lee, S. g. Lee; *Impact of Anions on Electrocatalytic Activity in Palladium Nanoparticles Supported on Ionic Liquid-Carbon Nanotube Hybrids for the Oxygen Reduction Reaction*, Chemistry - An Asian Journal **6** (2011) 2016-2021.

[25]. Y. S. Chun, J. Y. Shin, C. E. Song, S. g. Lee; *Palladium nanoparticles supported onto ionic carbon nanotubes as robust recyclable catalysts in an ionic liquid*, Chemical Communications (2008) 942-944.

[26]. J. Palomar, J. Lemus, M. A. Gilarranz, J. J. Rodriguez; *Adsorption of ionic liquids from aqueous effluents by activated carbon*, Carbon **47** (2009) 1846-1856.

[27]. A. J. Romero-Anaya, M. A. Lillo-Ródenas, C. Salinas-Martínez de Lecea, A. Linares-Solano; *Hydrothermal and conventional H_3PO_4 activation of two natural bio-fibers*, Carbon **50** (2012) 3158-3169.

[28]. F. Rodríguez-Reinoso, A. Linares-Solano; *Chemistry and physics of carbon* **21**, Marcel Dekker Inc. (1989) 1-146.

[29]. F. Rouquerol, J. Rouquerol, K. Sing; *Adsorption by powders & porous solids - Principles, Methodology and Applications*, Academic Press, London (1999)

[30]. D. Cazorla-Amorós, J. Alcañiz-Monge, A. Linares-Solano; *Characterization of activated carbon fibers by CO_2 adsorption*, Langmuir **12** (1996) 2820-2824.

[31]. D. Lozano-Castelló, D. Cazorla-Amorós, A. Linares-Solano; *Usefulness of CO_2 adsorption at 273 K for the characterization of porous carbons*, Carbon **42** (2004) 1231-1236.

[32]. H. P. Boehm; *Surface oxides on carbon and their analysis: a critical assessment*, Carbon **40** (2002) 145-149.

[33]. M. C. Román-Martínez, D. Cazorla-Amorós, D. Cazorla-Amorós, A. Linares-Solano, C. Salinas Martínez de Lecea; *TPD and TPR characterization of carbonaceous supports and Pt/C catalysts*, Carbon **31** (1993) 895-902.

[34]. G. S. Szymanski, Z. Karpinski, S. Biniak, A. Swiatkowski; *The effect of the gradual thermal decomposition of surface oxygen species on the chemical and catalytic properties of oxidized activated carbon*, Carbon **40** (2002) 2627-2639.

[35]. S. Haydar, C. Moreno-Castilla, M. A. Ferro-García, F. Carrasco-Marín, J. Rivera-Utrilla, A. Perrard, J. P. Joly; *Regularities in the temperature-programmed desorption spectra of CO_2 and CO from activated carbons*, Carbon **38** (2000) 1297-1308.

[36]. J. P. Marco-Lozar, D. Cazorla-Amorós, A. Linares-Solano; *A new strategy for germanium adsorption on activated carbon by complex formation*, Carbon **45** (2007) 2519-2528.

[37]. C. Moreno-Castilla, F. Carrasco-Marín, A. Mueden; *The creation of acid carbon surfaces by treatment with $(NH_4)_2S_2O_8$*, Carbon **35** (1997) 1619-1626.

[38]. C. Moreno-Castilla, M. V. López-Ramón, F. Carrasco-Marín; *Changes in surface chemistry of activated carbons by wet oxidation*, Carbon **38** (2000) 1995-2001.

[39]. Y. Qiao, F. Yan, S. Xia, S. Yin, P. Ma; *Densities and Viscosities of [Bmim][PF6] and Binary Systems [Bmim][PF6] + Ethanol, [Bmim][PF6] + Benzene at Several Temperatures and Pressures: Determined by the Falling-Ball Method*, Journal of Chemical & Engineering Data **56** (2011) 2379-2385.

[40]. M. Kosmulski, J. Gustafsson, J. B. Rosenholm; *Thermal stability of low temperature ionic liquids revisited*, Thermochimica Acta **412** (2004) 47-53.

[41]. L. y. Wang, Y. l. Xu, S. g. Jiang, M. g. Yu, T. x. Chu, W. q. Zhang, Z. y. Wu, L. w. Kou; *Imidazolium based ionic liquids affecting functional groups and oxidation properties of bituminous coal*, Safety Science **50** (2012) 1528-1534.

[42]. A. Triolo, A. Mandanici, O. Russina, V. Rodriguez-Mora, M. Cutroni, C. Hardacre, M. Nieuwenhuyzen, H. J. Bleif, L. Keller, M. A. Ramos; *Thermodynamics, structure, and dynamics in room temperature ionic liquids:the case of 1-butyl-3-methyl imidazolium hexafluorophosphate ([bmim][PF6])*, The Journal of Physical Chemistry B **110** (2006) 21357-21364.

[43]. S. Saouane, S. E. Norman, C. Hardacre, F. P. A. Fabbiani; *Pinning down the solid-state polymorphism of the ionic liquid [bmim][PF6]*, Chemical Science **4** (2013) 1270-1280.

[44]. M. Rufete-Beneite, C.C. Gheorghiu, M.C. Román-Martínez, C. Salinas-Martínez de Lecea, A. Linares-Solano; *Sistemas SILPC basados en materiales de carbono para hidrogenación asimétrica*, Annual Meeting SECAT(2013) 39-40.

[45]. J. L. Anthony, E. J. Maginn, J. F. Brennecke; *Solution thermodynamics of imidazolium-based ionic liquids and water*, Journal of Physical Chemistry B **105** (2001) 10942-10949.